

# Chiral dynamics in $\gamma p \rightarrow \pi^0 \eta p$ and related reactions

M. Döring<sup>1</sup>, E. Oset<sup>1</sup> and D. Strottman<sup>1,2</sup>

<sup>1</sup> Departamento de Física Teórica and IFIC, Centro Mixto Universidad de Valencia-CSIC, Institutos de Investigación de Paterna, Aptd. 22085, 46071 Valencia, Spain

<sup>2</sup> Theoretical Division, Los Alamos National Laboratory, Los Alamos, NM 87545

Using a chiral unitary approach for meson-baryon scattering in the strangeness zero sector, where the  $N^*(1535)$  and  $\Delta^*(1700)$  resonances are dynamically generated, we study the reactions  $\gamma p \rightarrow \pi^0 \eta p$  and  $\gamma p \rightarrow \pi^0 K^0 \Sigma^+$  at photon energies at which the final states are produced close to threshold. Among several reaction mechanisms, we find the most important is the excitation of the  $\Delta^*(1700)$  state which subsequently decays into a pseudoscalar meson and the  $N^*(1535)$ . Hence, the reaction provides useful information with which to test current theories of the dynamical generation of the low-lying  $1/2^-$  and  $3/2^-$  states. Predictions are made for cross sections and invariant mass distributions which can be compared with forthcoming experiments at ELSA.

PACS numbers: 25.20.Lj, 11.30.Rd

## I. INTRODUCTION

The unitary extensions of chiral perturbation theory  $U\chi PT$  have brought new light in the study of the meson-baryon interaction and have shown that some well known resonances qualify as dynamically generated, or in simpler words, they are quasibound states of a meson and a baryon, the properties of which are described in terms of chiral Lagrangians. After early studies in this direction explaining the  $\Lambda(1405)$  and the  $N^*(1535)$  as dynamically generated resonances [1, 2, 3, 4, 5], more systematic studies have shown that there are two octets and one singlet of resonances from the interaction of the octet of pseudoscalar mesons with the octet of stable baryons [6, 7]. The  $N^*(1535)$  belongs to one of these two octets and plays an important role in the  $\pi N$  interaction with its coupled channels  $\eta N$ ,  $K\Lambda$  and  $K\Sigma$  [8]. Here, we adopt and extend the ideas of Ref. [9] for the reaction  $\gamma p \rightarrow K^+ \pi \Sigma$  and study the analogous reaction  $\gamma p \rightarrow \pi^0 \eta p$  where the  $\eta p$  final state can form the  $N^*(1535)$  resonance. Besides processes relevant in  $\gamma p \rightarrow \pi \pi N$  [10], we also include [11] the contribution from the  $\Delta^*(1700)$  resonance which qualifies as dynamically generated through the interaction of the  $0^-$  meson octet and the  $3/2^+$  baryon decuplet as recent studies show [12, 13].

At the same time we also study the  $\gamma p \rightarrow \pi^0 K^0 \Sigma^+$  reaction and make predictions for its cross section, taking advantage of the fact that it appears naturally within the coupled channels formalism of the  $\gamma p \rightarrow \pi^0 \eta p$  reaction and leads to a further test of consistency of the ideas explored here. Both reactions are currently being analyzed at ELSA[14].

## II. ETA PION PHOTOPRODUCTION

Before turning to the two-meson photoproduction, we give a short review of the properties of the  $N^*(1535)$  in the meson-baryon sector, where this resonance shows up clearly in the spin isospin ( $S = 1/2, I = 1/2$ ) channel. The model of Ref. [8] provides an accurate data description of elastic and quasielastic  $\pi N$  scattering in the  $S_{11}$  channel. Within the coupled channel approach in the  $SU(3)$  representation of Ref. [8], not only the  $\pi N$  final state is accessible, but also  $K\Sigma$ ,  $K\Lambda$ , and  $\eta N$  in a natural way. The corresponding  $C_{ij}$  coefficients for the  $s$ -wave interaction kernel in the charge  $Q = +1$  sector are found in Ref. [11]. Besides the interaction from the lowest order chiral Lagrangian [15, 16, 17], also the  $\pi N \rightarrow \pi \pi N$  two loop contribution is included. In Ref. [11] it is shown that the same model for the resonance provides a good data description close to threshold for the one- $\eta$  photoproduction,  $\gamma p \rightarrow \eta p$ , when including some basic photoproduction mechanisms, which makes us confident to use the model of the  $N^*(1535)$  for the more complex reaction with two mesons in the final state in the next section.

### A. Production mechanisms for $\gamma p \rightarrow \pi^0 \eta p$

In Fig. 1 the relevant photoproduction mechanisms are shown. Diagrams (c) shows the pole terms that accompanies the contact term (b) in order to ensure gauge invariance. Similar terms are included for diagrams (a), (d), and (f) but not separately drawn. In all diagrams, the gray blob signifies the dynamically generated  $N^*(1535)$  that provides the final state interaction  $MB \rightarrow \eta p$  with the intermediate meson-baryon state in the loop given by the list of channels

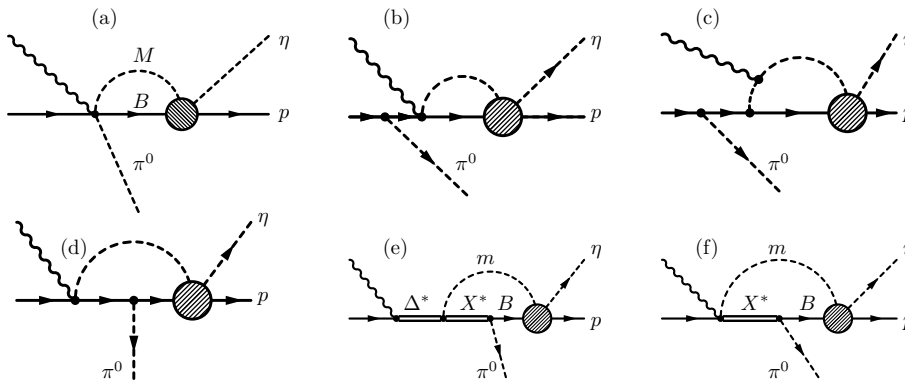


FIG. 1: Photoproduction mechanisms for the  $\pi^0\eta p$  final state.

from above. Here, we can only give a qualitative description of the processes and the amplitudes which are denoted in detail in Ref. [11].

Diagram (a) uses a contact term in a similar way as for the  $K^+\Lambda(1405)$  photoproduction in Ref. [9], additionally taking into account the anomalous magnetic moment of the nucleon with the effective Lagrangian from Ref. [18]. Diagrams (b) and (c) are a straightforward extension of the basic photoproduction mechanisms in  $\gamma p \rightarrow \eta p$  [11] for the final state with an additional  $\pi^0$ . It is known that the inclusion of explicit resonances plays an important role in the two-pion photoproduction [10], and therefore we include the relevant mechanisms as sub-processes in the calculation: In diagram (e) we show the contribution from the  $\Delta^*(1700)$  decay into  $X^* = \Delta(1232)$  and  $m = \pi$ . In the same way, the  $N^*(1520)$  decay from Ref. [10] is taken into account. Fig. (f) shows the corresponding  $\Delta$ -Kroll-Ruderman term ( $X^* = \Delta, m = \pi, B = N$ ) and also the  $\Sigma^*$ -Kroll-Ruderman term ( $X^* = \Sigma^*, m = K, B = \Lambda$ ). Additionally, we include the contribution from the dynamically generated  $3/2^-$  resonance from Ref. [13] which has been identified with the  $\Delta^*(1700)$ . In particular, the decay channels  $(mX^*B) = (\eta\Delta^+(1232)p), (K^+\Sigma^{*0}(1385)\Lambda), (K^0\Sigma^{*+}\Sigma^+)$  in diagram (e) are possible, whose strengths are not measured yet in experiment but a genuine prediction of the model [13]. From these couplings, also a tree level diagram originates for the photoproduction:  $\gamma p \rightarrow \Delta^*(1700) \rightarrow \eta\Delta^+(1232)[\pi^0 p]$ .

### III. NUMERICAL RESULTS

The invariant mass spectra for  $M_I(\eta p)$  and  $M_I(\pi^0 p)$  and cross section for the  $\gamma p \rightarrow \pi^0\eta p$  reaction are predicted which can be directly compared to the forthcoming experiments at the ELSA facility. In Fig. 2 the spectrum for  $M_I(\eta p)$  is shown for several lab photon energies  $E_\gamma$ , taking into account all processes from Fig. 1 plus the tree level process described at the end of Sec. II A. The solid and dashed curves correspond to the full and reduced model (no  $\pi N \rightarrow \pi\pi N$  channel, no vector exchange in  $t$ -channel, see Ref. [8], [11]) for the  $N^*(1535)$  resonance, and we take the difference as a hint for the theoretical error. The  $N^*(1535)$  is clearly visible in the spectrum, although it

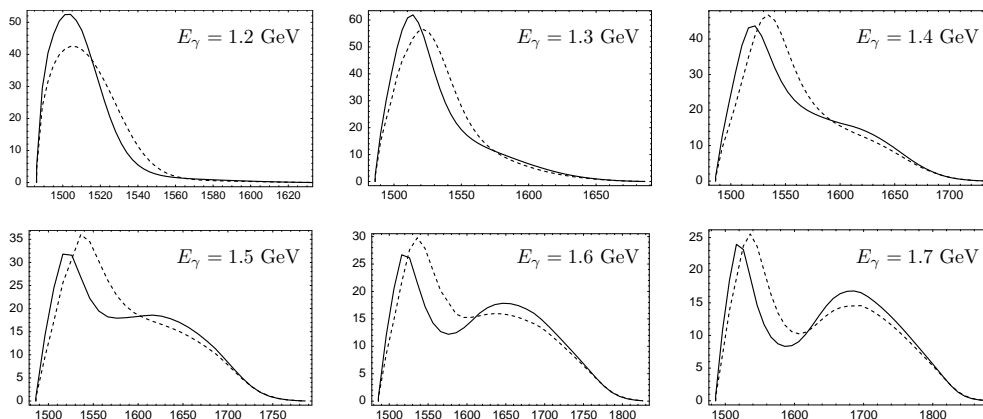


FIG. 2: Invariant mass spectrum  $\frac{d\sigma}{dM_I(\eta p)}$  [ $\mu\text{b GeV}^{-1}$ ] as a function of  $M_I(\eta p)$  [MeV] for various photon lab energies  $E_\gamma$ . Solid and dashed lines: Full and reduced model for the  $N^*(1535)$ , respectively.

interferes with the tree level process at low  $E_\gamma$  which shifts its position slightly. At higher  $E_\gamma$ , we observe a second peak which moves with the energy. This is a reflection of the  $\Delta(1232)$  in the tree level process which is on shell around these invariant masses. For a more detailed discussion, see Ref. [11]. The  $\pi^0 p$  invariant mass spectrum is not shown here, but in Ref. [11]. There, the  $\Delta(1232)$  shows up as a clean signal as expected. The total cross section is plotted in Fig. 3. Additionally to the full and reduced model, we show the outcome when using the phenomenological

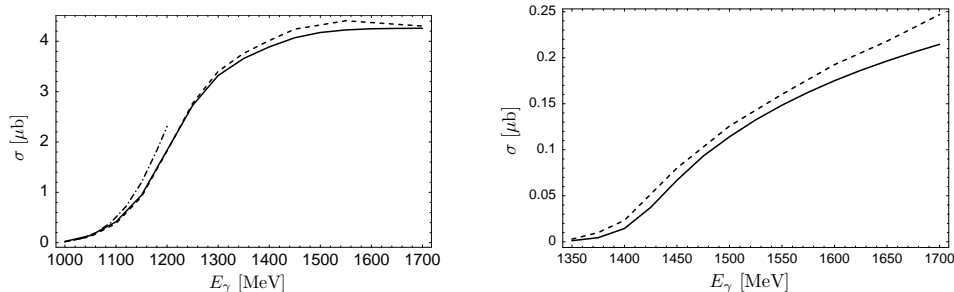


FIG. 3: Left side: Integrated cross section  $\sigma$  for the  $\gamma p \rightarrow \pi^0 \eta p$  reaction. Right side:  $\sigma$  for the  $\gamma p \rightarrow \pi^0 K^0 \Sigma^+$  reaction. Solid line: Full model for the  $N^*(1535)$ . Dashed line: Reduced model. Dashed dotted line (left side): Phenomenological potential for the  $MB \rightarrow \eta p$  transition (only available up to  $E_\gamma \sim 1.2$  GeV).

meson-baryon  $\rightarrow \eta p$  transition from the PWA from Ref. [19]. From the processes with  $N^*(1535)$ , diagram (e) from Fig. 1 with  $m = \eta$ ,  $X^* = \Delta(1232)$  gives the largest contribution which is due to the strong  $\eta p \rightarrow \eta p$  transition in the model for the  $N^*(1535)$ . Also, the tree level diagram contributes significantly as we have already seen in Fig. 2. The cross section is relatively independent of the chosen model for the  $N^*(1535)$  (solid vs. dashed line), and even the the phenomenological potential does not change much the result.

The  $\gamma p \rightarrow \pi^0 K^0 \Sigma^+$  reaction is calculated in a similar way as for the  $\pi^0 \eta p$  final state by replacing the  $\eta p$  final state of the  $N^*(1535)$  by the  $K^0 \Sigma^+$  one and including a new tree level diagram in analogy to the process described at the end of Sec. II A:  $\gamma p \rightarrow \Delta^*(1700) \rightarrow K^0 \Sigma^* + [\pi^0 \Sigma^+]$ . The cross section for  $\gamma p \rightarrow \pi^0 K^0 \Sigma^+$  is much smaller than for the  $\pi^0 \eta p$  final state as Fig. 3 shows. This is — among other reasons [11] — due to the fact that the reaction takes places at much higher photon energies where the dynamically generated  $N^*(1535)$  is off shell.

#### IV. CONCLUSIONS

In this paper we have studied the reactions  $\gamma p \rightarrow \pi^0 \eta p$  and  $\gamma p \rightarrow \pi^0 K^0 \Sigma^+$  within a chiral unitary framework which considers the interaction of mesons and baryons in coupled channels and dynamically generates the  $N^*(1535)$ . From the various processes, we find dominant the decay of the dynamically generated  $\Delta^*(1700)$  resonance into  $\eta \Delta$ , followed by the unitarization, or in other words, the  $\Delta^*(1700) \rightarrow \pi^0 N^*(1535)$  decay. A similar term provides also a tree level process which leads, together with the  $N^*(1535)$ , to a characteristic double hump structure in the  $\eta p$  and  $\pi^0 p$  invariant masses at higher photon energies.

A virtue of this approach and a test of the nature of the resonance as a dynamically generated object is that one can make predictions about cross sections for the production of the resonance without introducing the resonance explicitly in the formalism since only its components in the  $(0^-, 1/2^+)$  and  $(0^-, 3/2^+)$  meson-baryon base is what matters, together with the coupling of the photons to these components and their interaction in a coupled channel formalism. In particular, the reactions studied here probe decay channels of these resonances such as  $\Delta^*(1700) \rightarrow \eta \Delta$ ,  $\Delta^*(1700) \rightarrow K \Sigma^*$  or transitions like  $\eta p \rightarrow N^*(1535) \rightarrow \eta p$  which are predicted by the model and not measured yet.

The measurement of both cross sections is being performed at the ELSA/Bonn Laboratory and hence the predictions are both interesting and opportune and can help us gain a better insight in the nature of some resonances, particularly the  $N^*(1535)$  and the  $\Delta^*(1700)$  in the present case.

#### Acknowledgments

This work is partly supported by DGICYT contract number BFM2003-00856, and the E.U. EURIDICE network contract no. HPRN-CT-2002-00311. This research is part of the EU Integrated Infrastructure Initiative Hadron

Physics Project under contract number RII3-CT-2004-506078.

---

- [1] N. Kaiser, P. B. Siegel and W. Weise, Phys. Lett. B **362** (1995) 23.
- [2] N. Kaiser, T. Waas and W. Weise, Nucl. Phys. A **612** (1997) 297
- [3] E. Oset and A. Ramos, Nucl. Phys. A **635** (1998) 99
- [4] J. C. Nacher, A. Parreno, E. Oset, A. Ramos, A. Hosaka and M. Oka, Nucl. Phys. A **678** (2000) 187
- [5] J. A. Oller and U. G. Meissner, Phys. Lett. B **500** (2001) 263
- [6] D. Jido, J. A. Oller, E. Oset, A. Ramos and U. G. Meissner, Nucl. Phys. A **725** (2003) 181
- [7] C. Garcia-Recio, M. F. M. Lutz and J. Nieves, Phys. Lett. B **582** (2004) 49
- [8] T. Inoue, E. Oset and M. J. Vicente Vacas, Phys. Rev. C **65** (2002) 035204
- [9] J. C. Nacher, E. Oset, H. Toki and A. Ramos, Phys. Lett. B **455** (1999) 55
- [10] J. C. Nacher, E. Oset, M. J. Vicente and L. Roca, Nucl. Phys. A **695**, 295 (2001)
- [11] M. Doring, E. Oset and D. Strottman, arXiv:nucl-th/0510015.
- [12] E. E. Kolomeitsev and M. F. M. Lutz, Phys. Lett. B **585**, 243 (2004)
- [13] S. Sarkar, E. Oset and M. J. Vicente Vacas, Nucl. Phys. A **750**, 294 (2005)
- [14] V. Metag and M. Nanova, private communication.
- [15] J. Gasser and H. Leutwyler, Nucl. Phys. **B250** (1985) 465, 517, 539.
- [16] U. G. Meissner, Rep. Prog. Phys. 56 (1993) 903; V. Bernard, N. Kaiser and U. G. Meissner, Int. J. Mod. Phys. E4 (1995) 193.
- [17] G. Ecker, Prog. Part. Nucl. Phys. 35 (1995) 1.
- [18] D. Jido, A. Hosaka, J. C. Nacher, E. Oset and A. Ramos, Phys. Rev. C **66** (2002) 025203
- [19] R. A. Arndt, W. J. Briscoe, I. I. Strakovsky, R. L. Workman and M. M. Pavan, Phys. Rev. C **69**, 035213 (2004)